

A simple model for relating concentrations and fluctuations of trace reactive species to their lifetimes in the atmosphere

Donald H. Lenschow

National Center for Atmospheric Research (NCAR), Boulder, Colorado, USA

David Gurarie

Department of Mathematics, Case Western Reserve University, Cleveland, Ohio, USA

Received 10 May 2002; revised 13 August 2002; accepted 15 August 2002; published 28 December 2002.

[1] By means of a simple analytical one-dimensional (1-D) model, we predict mean vertical structure and fluctuations in trace gas concentrations as a function of species lifetime in the atmosphere. The model assumes a well-mixed planetary boundary layer (PBL) overlain by a free troposphere with constant diffusivity separated by a jump in species concentration. A jump in concentration is also assumed across the tropopause, and an exponential increase in diffusivity with height is assumed through the stratosphere. This three-layer model is applied to species with surface sources that have lifetimes of the order of days to years and predicts that the standard deviations of the concentration fluctuations normalized by the mean concentration are approximately proportional to the lifetimes of the trace gases to a power between $-1/2$ and -1 , depending on altitude and lifetime. Observations from several long-range aircraft field deployments, which collected gas samples from within the PBL up to 12 km altitude, generally agree with this prediction. A relation of this type is useful for estimating lifetimes of trace gases in the atmosphere or, conversely, if the lifetimes are known, average entrainment rates in the measurement region. The model also predicts a relationship among the surface emission, mean concentration, and lifetime, so that given any two of these quantities the third can be estimated.

INDEX TERMS: 0322 Atmospheric Composition and Structure: Constituent sources and sinks; 0368 Atmospheric Composition and Structure: Troposphere—constituent transport and chemistry; 3362 Meteorology and Atmospheric Dynamics: Stratosphere/troposphere interactions; 3367 Meteorology and Atmospheric Dynamics: Theoretical modeling; 3379 Meteorology and Atmospheric Dynamics: Turbulence; *KEYWORDS:* species lifetimes, chemical transport, atmospheric reactions, vertical exchange, global model

Citation: Lenschow, D. H., and D. Gurarie, A simple model for relating concentrations and fluctuations of trace reactive species to their lifetimes in the Atmosphere, *J. Geophys. Res.*, 107(D24), 4805, doi:10.1029/2002JD002526, 2002.

1. Introduction

[2] Many trace gases in the atmosphere are emitted into the planetary boundary layer (PBL) near or at the surface and destroyed by chemical reactions as they move about in the atmosphere. These processes generate fluctuations in the concentration, $S = \bar{S} + s$, where \bar{S} is the mean and s the fluctuation, which can be used to infer lifetimes of species, or alternatively, if the lifetimes are known, we may be able to infer transport properties of the atmosphere, or surface emission patterns. One way to study this is to analyze the variations of a suite of chemical species sampled at various locations and at various times. For example, an airplane can be used to collect samples of a suite of species during a flight, or series of flights, and the standard deviations of the species concentrations σ_s , obtained from the collection of samples, normalized by \bar{S} , can be calculated. An application of this is to estimate lifetimes of trace species which are

unknown by using a suite of species of different lifetimes τ to establish a relationship between σ_s/\bar{S} and τ . To the extent that the emission patterns and the sink processes are similar, we would expect a predictable relationship between σ_s/\bar{S} and τ . Similarly, we would expect a predictable relationship between S , τ , and total emission.

[3] Such a relationship between σ_s/\bar{S} and τ was apparently first described by Junge [1963, 1974] who suggested that σ_s/\bar{S} should be inversely proportional to τ , i.e.,

$$\sigma_s/\bar{S} = A\tau^{-\alpha} \quad (1)$$

with A a constant and $\alpha = 1$. His argument was based on the decay of the species as it is advected downstream from its source. Subsequent theoretical developments that attempt to predict a relation of this type have been based on either this type of argument, or on modeling the source and removal terms as stochastic variables. In subsequent sections, we review these different models, then develop a new analytical model based on a three-tiered structure of the atmosphere with parameterized exchange across the two layer inter-

faces. The model predictions are then compared to observations of mean concentrations and standard deviations based on grab-sample measurements of suites of chemical species from long-range aircraft-based observational studies.

2. Previous Models and Observations

[4] A variety of different models has appeared in the literature to predict the standard deviations of trace species as a function of species lifetime. These models are based on either deterministic equations that estimate the standard deviation on the basis of sampling protocols over finite spatial or temporal ranges, or on modeling the source and removal terms as stochastic variables. In the first case, the measurement can be considered from the perspective of either (1) measuring a time series at a particular location that, because of variability in the wind field and mixing processes, will sample air from a distribution of trajectories with varying source and removal histories or (2) measuring the spatial variability (e.g., by aircraft) downstream of a distribution of sources without regard to the small-scale structure of the wind field.

[5] We start with a generalized transport equation with both source and sink terms P and RS ,

$$\frac{\partial S}{\partial t} + \frac{1}{\rho} \nabla \cdot (\rho \vec{V} S) + RS = P, \quad (2)$$

where ρ is air density and \vec{V} is the velocity vector. One straightforward one-dimensional (1-D) limiting case for (1) is to assume a simple first-order decay process and negligible contribution by transport, modeled by $\partial S/\partial t + S/\tau = 0$ [Jaenicke, 1982] on a sampling interval $0 < t < T$ with negligible production of variance by the source term; that is, $\sigma_s = \sigma_P \gg \sigma_R$. This has the solution $S = S_0 e^{-t/\tau}$. The concentration and total variance are:

$$S = S_0 \frac{1 - e^{-T/\tau}}{T/\tau}, \quad (3)$$

and

$$\overline{S^2} = S^2 + \sigma_s^2 = S_0^2 \frac{1 - e^{-2T/\tau}}{2T/\tau}. \quad (4)$$

Hence,

$$\frac{\sigma_s^2}{S^2} = \frac{\overline{S^2}}{S^2} - 1 = \frac{T}{2\tau} \left(\frac{1 + e^{-T/\tau}}{1 - e^{-T/\tau}} \right) - 1 = \frac{T}{2\tau} \coth\left(\frac{T}{2\tau}\right) - 1, \quad (5)$$

and for $T \ll \tau$,

$$\frac{\sigma_s}{S} \approx \frac{T}{2\sqrt{3}} \tau^{-1}. \quad (6)$$

The coefficient $A = \frac{T}{2\sqrt{3}}$ corresponds to the Junge [1974] estimate of $A = 0.14$ years, if the sampling time $T \approx 0.48$ years. Furthermore, at the other limit, i.e., for $T \gg \tau$,

$$\frac{\sigma_s}{S} \approx \sqrt{\frac{T}{2}} \tau^{-1/2}. \quad (7)$$

[6] For (1), Slinn [1988] showed that assuming steady state horizontal advection by a mean flow U ,

$$U \frac{\partial S}{\partial x} + \frac{S}{\tau} = 0 \quad (8)$$

on the spatial interval $0 < x < L$ is equivalent to the time-dependent problem (1) with $t = x/U$. Thus it has the same form of σ_s/S with $T = L/U$. To get the Junge [1974] estimate of A , if we assume a mean transport velocity $U = 10 \text{ m s}^{-1}$, the required sampling distance downwind from the source is $L \approx 1300 \text{ km}$. (5) is similar to the results obtained by Hamrud [1983] using a 2-D numerical model with an eddy diffusivity that varied over the meridional cross section.

[7] For the stochastic approach, Gibbs and Slinn [1973] assumed stochastic source and removal terms, and wrote them as a sum of a mean and perturbation. They then separated the resulting equation into mean and fluctuating components, discarding terms with products of fluctuations and assumed exponential decorrelation with time for the fluctuations. In this case, $\sigma_s = \sigma_R + \sigma_P$. The approximate solution for the normalized variance for $T \gg \tau$ is $\sigma_s/S \propto \tau^{-1/2}$, which is in agreement with the deterministic case for large T . Thus, two very different processes have been invoked to conceptually model the standard deviation of nonconserved trace species to obtain $\alpha = 1/2$ for large τ . These simple models consider the atmosphere as one layer and do not take into account vertical structure.

[8] More recently, Ehhalt *et al.* [1998] developed a hierarchy of scalar diffusion models to illustrate aspects of diffusion of reactive species. They started with a simple 1-D model of steady state vertical diffusion with a constant turbulent diffusivity that illustrates the inherent property of a second-order diffusion equation to give a mean concentration that is proportional to $\tau^{1/2}$. They then showed, using 2-D and 3-D models, that for continental sources of species they could simulate fluctuations in species concentrations that followed (1) with $\alpha \simeq 0.5$. Their simple 1-D and 2-D models have constant vertical diffusivity.

[9] Definitive tests of these models using suites of chemical species spanning three or more decades of τ are only now being reported. Jobson *et al.* [1998, 1999], for example, have analyzed several archived data sets of quite extensive observations collected under different conditions and found that for measurements in the remote troposphere (i.e., far from localized sources), the value of α was about 1/2. Colman *et al.* [1999] used data from the NASA Pacific Exploratory Mission (PEM)-Tropics-A aircraft flights in 1996 to estimate the lifetime of CH_3Br , and obtained a value of α considerably less than one. Ehhalt *et al.* [1998] used data from PEM West B to infer the concentration of OH from the lifetimes of a suite of hydrocarbons which react with OH and found a value of $\alpha = 0.48$ for the hydrocarbons.

[10] Here, we develop a 1-D model, also using the concept of an eddy diffusion equation in the vertical, and add to this the process of mass exchange across the top of the PBL, as well as across the tropopause, to study in more detail the behavior of trace reactive species in the PBL, as well as the overlying free atmosphere. This 1-D global model, in contrast to previous models, assumes a horizontally homogeneous surface source, so the only source of

fluctuations is vertical exchange coupled with removal proportional to the mean concentration. We show that these processes can be a significant source of species fluctuation estimated, for example, by samples collected throughout an aircraft campaign, or by long-term observations at a fixed site. That is, by observations obtained over scales larger than the PBL turbulence scale. Thus, it is particularly relevant to measurements obtained in remote regions (such as over the ocean) characterized by horizontal homogeneity of both the meteorological and chemical environment. We also obtain relations among the net input, lifetime, and mean concentration and flux variations with height, both in the PBL and in the lower troposphere. Given global estimates of any two of these variables, the third can then be estimated. We do not consider modulation of the species lifetime by the diurnal cycle which might contribute to measurements of concentration fluctuations of very short-lived (e.g., less than a few days) photochemically reactive species.

[11] Advantages of this model include the simplicity of estimating both the means and fluctuations of trace species on a global scale, and the ease of modifying and extending the model to allow for changes in parameters and variables, such as specifying the lifetime as a function of height or adding time dependency. We see its primary application as a simple tool to explain observed means and standard deviations of trace species obtained from extended aircraft field deployments and from long-term observation sites in remote areas, and extending observations of species with known behavior (e.g., known lifetime) to species whose behavior is not known. Comparisons of model results with observations are, of course, dependent on the sampling protocol used to obtain the observations. Here we assume that the observations are obtained over space scales of hundreds of kilometers and timescales (for fixed-point measurements) of weeks to enable estimates of means and fluctuation levels relevant to the model predictions.

3. The Model

[12] The basis for this model is that mass exchange across the top of the PBL, as well as across the tropopause, can generate fluctuations in species concentrations in the PBL and free troposphere (i.e., the troposphere above the PBL) as observed by, for example, an aircraft flying at various altitudes and covering long distances, or a long-term observation site.

[13] We argue that for species with lifetimes greater than a few days, especially for those whose emission is relatively uniformly distributed horizontally the fluctuations in concentration in the PBL and lower free troposphere are generated mostly by transport across the PBL top. This process has previously been parameterized for generation of small-scale (scaling with the depth of the PBL) fluctuations in a horizontally homogeneous convective PBL via surface and entrainment fluxes by *Wyngaard and Brost* [1984] and *Moeng and Wyngaard* [1989]. Here we extend this concept to larger horizontal scales and to the entire troposphere. We argue that horizontally heterogeneous processes on the mesoscale (roughly ten to a thousand kilometers) in the troposphere, such as deep convection and frontogenesis, can generate fluctuations on these scales in the PBL which can

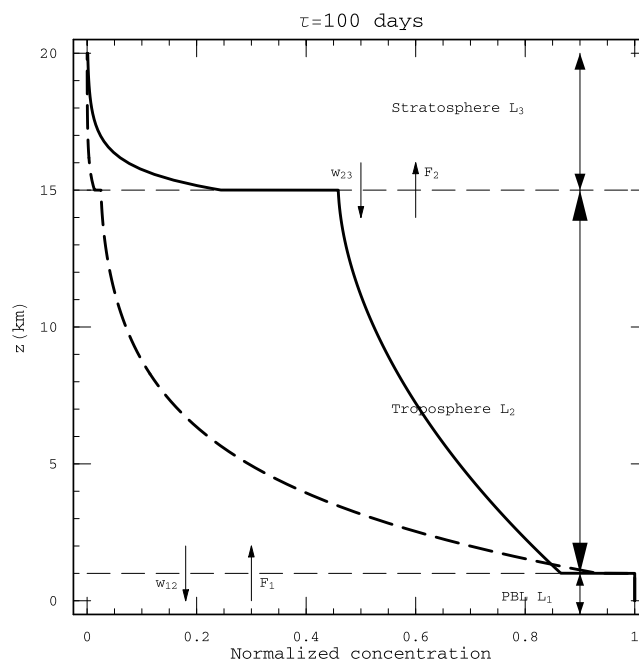


Figure 1. Modeled vertical profiles from the surface up into the stratosphere of a reactive species released in the PBL with a lifetime $\tau = 100$ days for values of $K_2 = 10 \text{ m}^2 \text{ s}^{-1}$ (solid line) and $K_2 = 1 \text{ m}^2 \text{ s}^{-1}$ (dashed line) normalized by the PBL concentration.

be of the same magnitude as the jumps in concentration across the PBL top [*Lenschow et al.*, 1999]. Fluctuations on these larger scales take longer to dissipate. Similarly, in the free troposphere fluctuations can occur which scale with some combination of the jumps across the PBL top, across the free troposphere, and across the tropopause. Here there is even less turbulence to dissipate the fluctuations.

[14] We parameterize this by constructing a model which consists of three layers (Figure 1): a lower layer (L_1) that is well mixed by direct interactions with the surface, assumed to be 1 km deep (the PBL); a middle layer (L_2), which is the rest of the troposphere extending to 15 km and capped by the tropopause, where vertical transport is characterized by a constant diffusivity; and an overlying layer (L_3), the stratosphere, assumed to extend to infinity and described by a diffusivity which increases with height. Each of these layers is assumed to be separated by a discontinuous change in concentration across an interface where the transport from the overlying to the underlying layer is assumed to occur via an exchange velocity times a change in concentration across the interface. This is assumed to be compensated by cumulus convection that intermittently transports air from the underlying to the overlying layer. The top of the PBL is the base of cumulus clouds that vent PBL air into the overlying free troposphere. These processes are schematically illustrated in Figure 2.

[15] Deep convective clouds can reach up to the tropopause, and occasionally penetrate into the stratosphere, transporting tropospheric air into the stratosphere (and vice versa) [e.g., *Danielsen*, 1982, 1993; *Holton et al.*, 1995]. The similarity of tropopause structure (including a jump in potential temperature across the tropopause) to that at the

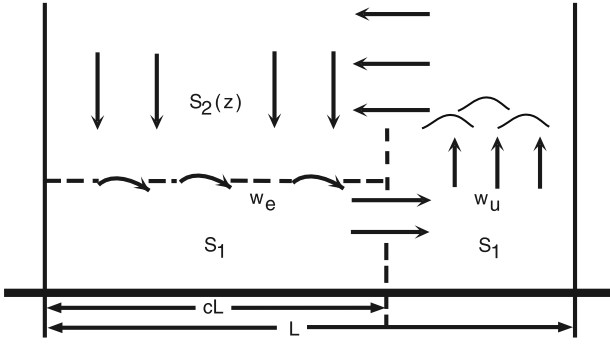


Figure 2. Schematic of the entrainment process at the top of the PBL and its compensation by cumulus convection.

top of the PBL has been noted by *Birner et al.* [2002]. Exchange of air between the troposphere and stratosphere also takes place by horizontal advection across breaks in the tropopause. The essence of the model is that the exchanges across both interfaces will generate concentration fluctuations in the adjoining layers that are proportional to the concentration differences between the two layers.

3.1. Governing Equations

[16] We model the diffusion-relaxation processes for the concentration of a species $S(z, t)$ with an atmospheric lifetime τ with a second-order parabolic differential equation,

$$\frac{\partial S}{\partial t} = \frac{1}{\rho} \frac{\partial}{\partial z} \rho K(z) \frac{\partial S}{\partial z} - \frac{S}{\tau}. \quad (9)$$

This can be derived from (2) by assuming horizontal homogeneity and using the concept of an eddy diffusivity for parameterizing the vertical turbulent transport.

[17] We denote the concentrations, diffusivities and air densities of the three layers by $S_i(z)$; K_i ; ρ_i ($i = 1, 2, 3$), the interfaces by z_1, z_2 , and the fluxes across z_1, z_2 by F_1, F_2 . The concentration at an interface we denote by S_i , and throughout the layer L_i by $S_i(z)$. Here we consider only steady state solutions, so (9) becomes an ordinary differential equation (ODE) on the half-line, solved separately for the three layers L_1, L_2 , and L_3 . The variables $\rho(z), K(z)$ take on different forms in L_1, L_2, L_3 as indicated in Table 1. The separate solutions for each layer are then matched at the boundaries via the prescribed flux boundary conditions. The fluxes F_1, F_2 are specified as the concentration differences across the boundary times an entrainment velocity,

$$F_1 = w_{12}(S_1 - S_2(z_1)); \quad \text{and} \quad F_2 = w_{23}(S_2(z_2) - S_3(z_2)). \quad (10)$$

The flux is conserved across the boundary and assumed to be diffusive away from the boundary; therefore, we have two boundary conditions at each interface z_i :

$$F_i = -K_i \frac{\partial S_i}{\partial z} = -K_{i+1} \frac{\partial S_{i+1}}{\partial z} = w_{i,i+1}(S_i - S_{i+1}). \quad (11)$$

In the PBL, mixing is relatively so efficient that we let $K_1 \rightarrow \infty$.

[18] Combining these conditions with the top and bottom boundary conditions, which are a prescribed surface flux F_0 at $z = 0$, and vanishing flux $\frac{\partial S_3}{\partial z} = 0$ at $z \rightarrow \infty$, we get a well-posed problem, whose (unique) solution describes the stationary distribution of the tracer concentration throughout the three layers. The three layers have different diffusion-relaxation regimes (different formulations for $K_i(z)$; $\rho_i(z)$), hence different solutions, as summarized in Table 1.

[19] The first three rows in Table 1 give expressions for the basic parameters in the set of differential equations for the three layers. Here we consider only a constant τ , but point out that it is straightforward to specify different values of τ for each layer, or even variation of τ with height, as for example, for photochemically active species or for reactions among species with varying concentrations with height.

[20] For L_1 we assume a perfectly mixed PBL ($K_1 \rightarrow \infty$) and $\tau \gg z_1/w_*$, where w_* is the convective velocity scale, defined by

$$w_* \equiv \left(\frac{g}{T} F_{Tv} z_1 \right)^{1/3} \quad (12)$$

where g/T is the buoyancy parameter and F_{Tv} is the surface virtual temperature flux. That is, the lifetime is assumed to be much greater than the mixing timescale within the PBL, which is typically less than an hour. Then (9) reduces to

$$\frac{\partial F}{\partial z} = -\frac{S_1}{\tau}. \quad (13)$$

Integrating (13) from the surface to the top of the PBL z_1 we obtain

$$F_1 - F_0 = -\frac{z_1}{\tau} S_1. \quad (14)$$

[21] For L_2 (the free troposphere), we assume a constant eddy diffusivity K_2 . Substituting the diffusive flux $F_2(z) = -K_2 \frac{\partial S_2}{\partial z}$ into (9), we obtain

$$\frac{1}{\rho} \frac{\partial}{\partial z} \rho K_2 \frac{\partial S_2(z)}{\partial z} - \frac{1}{\tau} S_2(z) = 0. \quad (15)$$

[22] The concept of an eddy diffusivity in the free troposphere is not very robust because much of the vertical

Table 1. Expressions for the Reaction Rate, Diffusivity, and Air Density As Well As the ODEs and Their Solutions for Each Atmospheric Layer Along With Expressions for the Parameters Used in the Solutions

	L_1	L_2	L_3
Reaction rate	$1/\tau$	$1/\tau$	$1/\tau$
Diffusion	∞	K_2 (constant)	$K_3(z_2) e^{k(z-z_2)}$
Density	ρ_0 (constant)	$\rho(z_1) e^{-l_2(z-z_1)}$	$\rho(z_2) e^{-l_3(z-z_2)}$
ODE (=0)	\dots	$S - l_2 S' - \frac{S}{\tau K_2}$	$S - (l_3 - k) S' - \frac{e^{-k(z-z_2)} S}{\tau K_3(z_2)}$
ODE solution	S_1	$c_1 y_1(z) + c_2 y_2(z)$	$c_3 y_3(z)$
$\{y_i(z)\}$	\dots	$\{e^{\lambda_1(z-z_1)}, e^{\lambda_2(z-z_2)}\}$	$e^{a(z-z_2)} I_\nu \left(\frac{2\sqrt{b}}{k} e^{-\frac{k}{2}(z-z_2)} \right)$
Parameters	\dots	$\lambda_{1,2} = \frac{l_2 \pm \sqrt{l_2^2 + \frac{1}{\tau K_2}}}{2}$	$a = l_3 - k; b = \frac{1}{k \sqrt{K_3(z_2) \tau}}$
			$\nu = \frac{l_3 - k}{k}$

transport occurs by processes other than small-scale turbulent eddies transferring mass from one adjacent level to another. Therefore, estimating the “best” mean value to characterize this transport is open to considerable conjecture. Suggested values in the literature range from about 1 to about $20 \text{ m}^2 \text{ s}^{-1}$ [Olofsson, 1988]. Although the range of K_2 makes considerable difference in the mean profiles, as we will show later, varying K_2 between 1 and $10 \text{ m}^2 \text{ s}^{-1}$ makes little difference in our conclusions.

[23] We use the approximation that $\rho \simeq \rho(z_1)^{-\ell_2(z-z_1)}$, where $\ell_2 = 0.1134 \times 10^{-3} \text{ m}^{-1}$ (i.e., a density scale height $\ell^{-1} = 8.82 \text{ km}$) for a standard troposphere, so that (15) becomes

$$\frac{\partial^2 S_2(z)}{\partial z^2} - \ell_2 \frac{\partial S_2(z)}{\partial z} - \frac{1}{K_2 \tau} S_2(z) = 0. \quad (16)$$

The solution to (16) can be expressed as the sum of two exponential terms, $S_2 = c_1 y_1(z) + c_2 y_2(z)$, $\{y_i(z) = e^{\lambda_i(z-z_1)}\}$ with as yet undetermined coefficients $\{c_1, c_2\}$.

[24] For L_3 (the stratosphere and above), we assume $K_3(z) = K_3(z_2) e^{k(z-z_2)}$, where $K_3(z_2) = 0.0711 \text{ m}^2 \text{ s}^{-1}$ and $k = 0.103 \times 10^{-3} \text{ m}^{-1}$ [Liley, 1995]. For density, we assume a standard isothermal stratosphere, with $\ell_3 \simeq 0.157 \times 10^{-3} \text{ m}^{-1}$. Then,

$$\frac{\partial^2 S_3(z)}{\partial z^2} - a \frac{\partial S_3(z)}{\partial z} - b e^{-k(z-z_2)} S_3(z) = 0, \quad (17)$$

where $a = \ell_3 - k$ and $b = 1/[K_3(z_2)\tau]$. The solution is given in terms of the modified Bessel functions $I_{\pm\nu}$ of order $\nu = \frac{a}{k}$,

$$S_{\pm}(z) = e^{\frac{a}{k}(z-z_2)} I_{\pm\nu} \left(\frac{2\sqrt{b}}{k} e^{-\frac{k}{2}(z-z_2)} \right), \quad (18)$$

Solutions S_{\pm} (of positive and negative order ν) have different asymptotes at $z \rightarrow \infty$: $y_3(z) = S_+(z) \sim \left\{ 1 + \frac{b}{(2+\nu)k^2} e^{-k(z-z_2)} + \dots \right\}$, which is regular, and $S_-(z) \sim e^{a(z-z_2)} \left\{ 1 + \frac{b}{(2-\nu)k^2} e^{-k(z-z_2)} + \dots \right\}$, which is singular. The regular solution (of positive order ν) $y_3 = S_+$ satisfies the zero-flux boundary condition at $z \rightarrow \infty$.

[25] Having obtained solutions $\{y_1, y_2, y_3\}$ of the ODEs in layers L_2, L_3 , and constant S_1 in L_1 , we can now determine the concentration profile through the entire atmosphere

$$S(z) = \begin{cases} S_1 & \text{in } L_1 \\ c_1 y_1(z) + c_2 y_2(z) & \text{in } L_2 \\ c_3 y_3(z) & \text{in } L_3 \end{cases} \quad (19)$$

in terms of four undetermined parameters $\{S_1, c_1, c_2, c_3\}$ that can be evaluated from the four boundary conditions (10) and (11) at z_1, z_2 . That is, the flux $-K_2 \frac{\partial S_2(z)}{\partial z}$ into L_2 at the z_1 interface equals the flux out of the PBL, $F_1 = F_0 - \frac{z_1}{\tau} S_1 = w_{12}(S_1 - S_2)$. Similarly at the z_2 interface, the flux $-K_3 \frac{\partial S_3(z)}{\partial z} \Big|_{z_2} = -K_2 \frac{\partial S_2(z)}{\partial z} \Big|_{z_2} = w_{23}(S_2 - S_3)$.

[26] The result is a linear algebraic system of four equations for $\{S_1, c_1, c_2, c_3\}$ involving the three ODE solutions $\{y_i\}$ and the parameters K_i and w_{ij} ,

$$\frac{z_1}{\tau} S_1 + K_2 y_1' \Big|_{z_1} c_1 + K_2 y_2' \Big|_{z_1} c_2 = F_0 \quad (20a)$$

$$w_{12} S_1 + (K_2 y_1' - w_{12} y_1) \Big|_{z_1} c_1 + (K_2 y_2' - w_{12} y_2) \Big|_{z_1} c_2 = 0 \quad (20b)$$

$$K_2 y_1' \Big|_{z_2} c_1 + K_2 y_2' \Big|_{z_2} c_2 - K_3 y_3' \Big|_{z_2} c_3 = 0 \quad (20c)$$

$$w_{23} y_1 \Big|_{z_2} c_1 + w_{23} y_2 \Big|_{z_2} c_2 + (K_3 y_3' - w_{23} y_3) \Big|_{z_2} c_3 = 0, \quad (20d)$$

where $(\sim)'$ denotes $\frac{\partial(\sim)}{\partial z}$.

[27] Having specified the diffusivities $\{K_i\}$ and the ODE solutions $\{y_i\}$ in all three layers, we now estimate the entrainment velocities w_{ij} across the two interfaces. At the top of the PBL, we estimate the entrainment velocity (10) from the Earth's surface energy budget (neglecting shear). Sellers [1965] estimated the average sensible energy flux over land and ocean as 31.9 and 10.6 W m^{-2} , respectively, and the corresponding latent energy fluxes as 33.2 and 98.3 W m^{-2} , respectively, with 70.8% of the Earth covered by ocean. This leads to an average surface virtual temperature flux of $0.019 \text{ m s}^{-1} \text{ K}$. We apply the simple Tennekes [1973] mixed-layer model to estimate the jump in temperature across the PBL top,

$$T_2 - T_1 \simeq \frac{\gamma z_1}{2 + m^{-1}}, \quad (21)$$

where $-m$ is the ratio of virtual temperature flux at z_1 to the surface flux and γ is the lapse rate of potential temperature just above z_1 . Here we assume $m = 0.2$ and $\gamma = 6.5 \text{ K km}^{-1}$ [Tennekes, 1973]. Using (10), which holds for any scalar including temperature, (21), and the surface virtual temperature flux, we obtain $w_{12} \simeq 0.0040 \text{ m s}^{-1}$. This gives a tropospheric turnover time with respect to the PBL of about 23 days.

[28] We can compare this estimate with a completely independent estimate obtained from consideration of the amount of air transported from the PBL to the troposphere by convective clouds. By continuity, the amount of mass entrained by the PBL should be equal to that transported by penetrating cumulus convection driven by latent heating (see Figure 2). We can obtain global estimates of both the mass of air vented out of the PBL by convection and the fractional area covered by this convective transport from the study of Cotton *et al.* [1995]. Their estimates of the area covered by precipitating clouds is $8.2 \times 10^{13} \text{ m}^2$, or about 16% of the Earth's surface, and for cloud mass flux about $4.95 \times 10^{19} \text{ kg yr}^{-1}$. This gives an average updraft velocity at $z_1 = 1 \text{ km}$ of $w_u = 0.017 \text{ m s}^{-1}$. Equating the air transported by cumulus convection to that entrained at the PBL top gives an entrainment velocity of

$$w_{12} = \frac{1-c}{c} w_u = 0.0033 \text{ m s}^{-1}, \quad (22)$$

where $c = 1 - 0.16 = 0.84$ is the fractional area of that part of the PBL that is entraining air. Although we use the

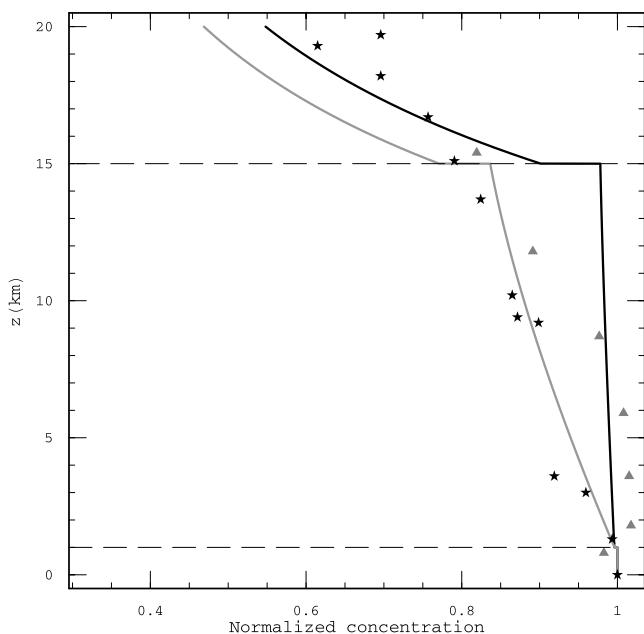


Figure 3. ^{85}Kr profile data obtained from the studies of *Telegadas and Ferber* [1975] (triangles) and *Levin and Hesshaimer* [1996] (stars) along with modeled concentration ($\tau = 15.52$ years) using $K_2 = 10 \text{ m}^2 \text{ s}^{-1}$ (black line) and $K_2 = 1 \text{ m}^2 \text{ s}^{-1}$ (gray line).

estimate of $w_{12} = 0.004 \text{ m s}^{-1}$ obtained from the surface buoyancy flux, it is comforting that (22) is in reasonable agreement with it.

[29] At the top of the troposphere, we estimate the entrainment velocity w_{23} from the estimate of *Holton et al.* [1995] of a 2-year turnover time of air above the 100 hPa level. This leads to an exchange velocity of $w_{23} \approx 10^{-4} \text{ m s}^{-1}$.

[30] Thus, we have determined all of the coefficients in the set of four equations ((20a), (20b), (20c), and (20d)), which can now be solved.

4. Results

[31] This simple analytical model allows us to easily investigate globally averaged behavior of trace reactive species. One difficulty in this approach is that approximating the transport through the troposphere as a diffusion process has long been known to be rather crude [e.g., *Hunten, 1975*].

[32] One source of information for estimating K_2 is vertical profiles of ^{85}Kr , which is predominantly emitted by nuclear power facilities and has a half-life of 10.76 years (i.e., $\tau = 15.52$ years). Unfortunately, measurements of profiles through the troposphere are rare. *Telegadas and Ferber* [1975] present a set of measurements obtained over the contiguous United States from January to June 1973, and *Levin and Hesshaimer* [1996] present measurements obtained over southern France “normalized to 1 January 1986.” In an attempt to determine what is the best value to use for K_2 , we have plotted the ^{85}Kr profile measurements from the studies of *Telegadas and Ferber* [1975] and *Levin and Hesshaimer* [1996] in Figure 3 along with the

modeled profiles for $K_2 = 1$ and $10 \text{ m}^2 \text{ s}^{-1}$. We see that it is not possible to unequivocally estimate any kind of “best fit” to these data. This is likely due to a combination of very limited (both spatially and temporally) data and shortcomings in applying the eddy diffusion concept to the free troposphere. Depending on what criteria are used, one could argue for any value between $K_2 = 1$ and $10 \text{ m}^2 \text{ s}^{-1}$. Based on a variety of studies of both radioactive and chemically reactive tracers, *Massie and Hunten* [1981] recommended a value of $10 \text{ m}^2 \text{ s}^{-1}$. Here we consider $K_2 = 1$ and $10 \text{ m}^2 \text{ s}^{-1}$ as plausible estimates of the range of K_2 in much of the subsequent analyses. Figure 1 shows concentration profiles for $\tau = 100$ days using both values of K_2 . Later we will show that for the objectives of this paper, the results are not particularly sensitive to the exact value of K_2 .

[33] Figure 4 is a plot of the concentration as a function of height normalized by the PBL concentration S_1 for $K_2 = 10 \text{ m}^2 \text{ s}^{-1}$ and $\tau = 1, 10, 10^2, 10^3$, and 10^4 days. We see that for $\tau = 1$ day, the normalized concentration drops rapidly above the PBL to a negligible value at about 5 km height, while at the other extreme, for $\tau = 10^4$ days the concentration is about 0.98 just below the tropopause. Also, at z_1 , $\Delta S_1/S_1 \equiv [S_1 - S_2(z_2)]/S_1$ decreases from about 0.27 at 1 day to almost zero at 10^4 days, while at z_2 , $\Delta S_2/S_2(z_2) \equiv [S_2(z_2) - S_3(z_2)]/S_2(z_2)$ is about 0.06 at 10^4 days.

4.1. Scalar Standard Deviation in the PBL

[34] We assume that exchanges between the free troposphere and the PBL are a primary cause of fluctuations in the PBL, and thus that $\Delta S_1 \propto \sigma_s$. Figure 5 shows a plot of $\Delta S_1/S_1$. For τ less than a few hundred days, the power law dependency of $\Delta S_1/S_1$ on τ steadily decreases and approaches $\alpha = 1$ for $\tau >$ about 500 days. However, in the range of τ varying between a few days to a few years,

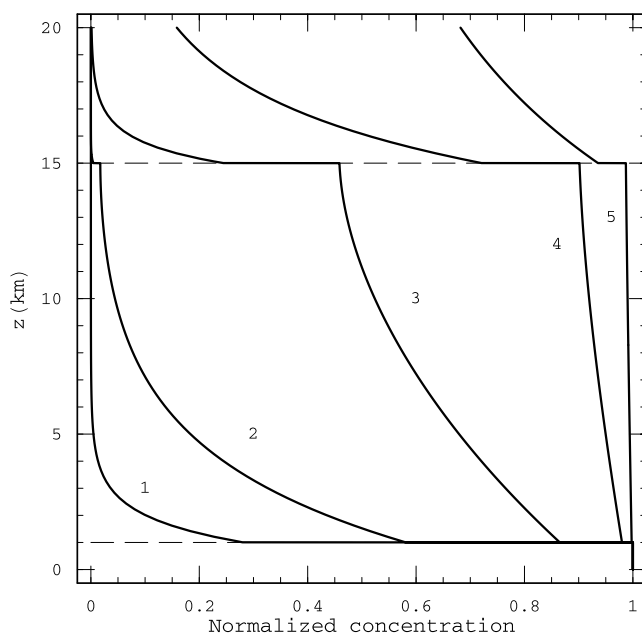


Figure 4. Species concentration versus height for $K_2 = 10 \text{ m}^2 \text{ s}^{-1}$ for various species lifetimes. Curves 1–5 are for $\tau = 1, 10, 10^2, 10^3$, and 10^4 days, respectively.

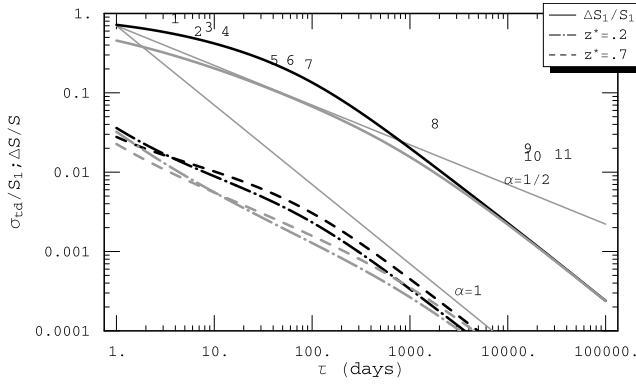


Figure 5. Plots of the normalized standard deviation of species concentration as a function of lifetime using the top-down and bottom-up diffusion formulation of *Moeng and Wyngaard* [1989] for two values of $z^* = z/z_1$ as well as the relation for normalized jump across the PBL top, $\Delta S_1/S_1 = [S_1 - S_2(z_1)]/S_1$, which is predicted by the model presented here for $K_2 = 10 \text{ m}^2 \text{ s}^{-1}$ (black lines) and for $K_2 = 1 \text{ m}^2 \text{ s}^{-1}$ (gray lines). The integers are observations of the standard deviation of the logarithm of species mixing ratios obtained from the study of *Jobson et al.* [1999] for aircraft measurements over the Hudson Bay lowlands and northern Quebec, Canada, from ABLE 3B: 1, *n*-butane; 2, benzene; 3, propane; 4, acetylene; 5, ethane; 6, C_2Cl_4 ; 7, CHCl_3 ; 8, CH_3CCl_3 ; 9, CCl_4 ; 10, CFC-11; and 11, CFC-12. The thin lines of slopes of $-1/2$ and -1 are drawn for reference.

the average slope can be approximated by $\alpha \approx 1/2$. For values of τ greater than a few years, the normalized jump becomes small, and difficult to measure in the PBL. The curves obtained here are very similar in shape to those obtained by *Hamrud* [1983] for uniform source and sink and by *Slinn* [1988] in that they both approach a slope of -1 for large τ , and have a slope closer to $-1/2$ for small τ , with a transition in the region of 10–1000 days. However, the magnitude of their coefficient A for the -1 regime is about 3 times larger than ours.

[35] Scalar fluctuations in an idealized horizontally homogeneous convective PBL are generated by fluxes at the surface and top of the PBL. These fluctuations scale with the size of the turbulent eddies generated by the surface buoyancy flux, which scale with the depth of the PBL. That is, the peak wavelength in the scalar variance spectrum (multiplied by wave number) generated by this process is about equal to the depth of the PBL [e.g., *Leschow*, 1995]. This concept of top-down and bottom-up scalar diffusion in the convective PBL was developed by *Wyngaard and Brost* [1984]. The top-down and bottom-up formulation obtained from large-eddy simulation of the convective PBL by *Moeng and Wyngaard* [1989] predicts that

$$\sigma_{td}^2 = \left(\frac{F_1}{w_*}\right)^2 f_t(z/z_1) + \left(\frac{F_0}{w_*}\right)^2 f_b(z/z_1) + 2 \frac{F_0 F_1}{w_*^2} f_{ib}(z/z_1) \quad (23)$$

where $f_t(z/z_1)$ is the top-down variance function

$$f_t(z/z_1) \simeq 3.1(1 - z/z_1)^{-3/2}, \quad (24)$$

$f_b(z/z_1)$ is the bottom-up function

$$f_b(z/z_1) \simeq (z/z_1)^{-0.9}, \quad (25)$$

and $f_{ib}(z/z_1)$ is the covariance function

$$f_{ib}(z/z_1) \simeq 0.5(f_t f_b)^{1/2}. \quad (26)$$

[36] Substituting (10), (24), (25), and (26), as well as S_1 and S_2 from the solution to (20a), (20b), (20c), and (20d) into (23) yields a relation for σ_{td}/S_1 , which is plotted in Figure 5 for $z^* \equiv z/z_1 = 0.2$ and 0.7 . The results show that the standard deviation predicted by the top-down and bottom-up formulation of *Moeng and Wyngaard* [1989] is more than an order of magnitude less than the model predictions for $\Delta S_1/S_1$ observed over the same range of τ , but with a very similar τ dependency. Of course, the real world is not horizontally homogeneous. Variations exist in both the sources and sinks of species, as well as the mean and turbulent structure of the atmosphere so the result is not particularly surprising. However, *Moeng and Wyngaard* [1989] do provide a baseline for estimating the fractional contribution of horizontally homogeneous processes to fluctuations observed in the PBL. Our model extends this to estimating the contribution due to mesoscale atmospheric processes that can introduce variability on scales larger than the PBL depth. Since the timescale for dissipation of scalar variance is proportional to the length scale of the eddies [*Tennekes and Lumley*, 1972], mesoscale eddies can persist for a proportionally longer time, and thus their contribution to the variance can extend further away from their origin.

[37] We have also plotted in Figure 5 the standard deviation of the logarithm of species mixing ratios obtained from the study of *Jobson et al.* [1999] for aircraft measurements over the Hudson Bay lowlands and northern Quebec, Canada, from Arctic Boundary Layer Expedition 3B (ABLE 3B). This measure of species fluctuation is very similar to the normalized standard deviation, and becomes increasingly close to it for large τ . We selected this data set because the observations are in the lower troposphere over a remote region. For $\tau < 100$ days, the measurements agree well with the $K_2 = 10 \text{ m}^2 \text{ s}^{-1}$ curve. For $\tau > 100$ days, the measurements continue to follow the $\alpha = 1/2$ curve, while the model approaches $\alpha = 1$.

[38] *Leschow et al.* [1999] found from analysis of 1-min samples of several photochemically active species emitted by the ocean collected during NASA PEM-Tropics-A in the tropical marine PBL (CH_3I , CHBr_3 , CH_3ONO_2 , and $\text{C}_2\text{H}_5\text{ONO}_2$) that their normalized standard deviations were much larger than predicted by top-down and bottom-up based on their estimated lifetimes in the PBL.

[39] Therefore, we conclude that values of σ_s in the PBL result not only from small-scale turbulent mixing in an assumed horizontally homogeneous PBL, as parameterized in (23), but also from mesoscale circulations that exchange air between L_1 and L_2 , and mesoscale variability in the entrainment rate and PBL height. These larger-scale exchange processes cannot mix out as rapidly as small-scale exchange [*Leschow et al.*, 1999], so we expect that σ_s is more directly related to the concentration difference between the two layers. Furthermore, we expect that larger

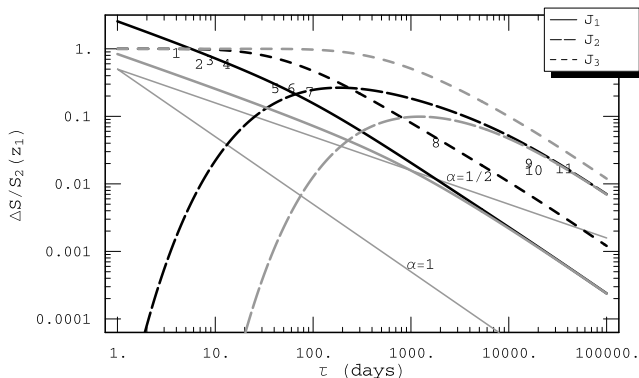


Figure 6. Modeled concentration differences normalized by the concentration just above the PBL versus lifetime τ for $K_2 = 10 \text{ m}^2 \text{ s}^{-1}$ (black lines) and for $K_2 = 1 \text{ m}^2 \text{ s}^{-1}$ (gray lines). $J_1 = (S_1 - S_2(z_1))/S_2(z_1)$ is the normalized jump in concentration across the PBL top, $J_2 = (S_2(z_2) - S_3(z_2))/S_2(z_1)$ is the normalized jump across the tropopause, and $J_3 = (S_2(z_1) - S_2(z_2))/S_2(z_1)$ is the normalized difference in concentration across the troposphere. The integers are data points obtained from the study of *Jobson et al.* [1999], as described in the caption for Figure 5. The thin reference lines have slopes of -1 and $-1/2$.

fluctuations may exist in L_2 than L_1 since mixing is less and S can vary with height in L_2 . Therefore, as suggested by *Lenschow et al.* [1999], we parameterize the standard deviation by

$$\sigma_s = C[S_1 - S_2(z_2)] \quad (27)$$

where C is a constant ≤ 1 in the PBL. We also point out that larger-scale horizontal fluctuations in PBL concentration eventually are broken down into smaller-scale fluctuations by PBL turbulence [*Kimmel et al.*, 2002].

[40] In the troposphere above the PBL we assume that concentration fluctuations measured in this region result from a combination of air exchanges: between the PBL and the overlying air, between the stratosphere and troposphere, and between different levels within the troposphere. These concentration differences, normalized by the concentration just above the PBL, are plotted in Figure 6. For $\tau < 100$ days, the average jump across the PBL top J_1 has a slope of $\approx -1/2$, while the jump across the troposphere $J_3 \rightarrow 1$ and the jump across the tropopause $J_2 \rightarrow 0$. For $K_2 = 10 \text{ m}^2 \text{ s}^{-1}$ and $200 < \tau < 2000$, as well as for $K_2 = 1 \text{ m}^2 \text{ s}^{-1}$ and $1000 < \tau < 10,000$, the jump across the tropopause J_2 has a slope $\approx -1/2$. For $\tau > 10,000$ days, J_1 , J_2 , and J_3 all approach a slope of -1 .

[41] If we look at the envelope of the magnitude of the jumps that we propose contribute to σ_s/S in the troposphere, especially in the regions where a particular jump exceeds the other two, and assume that $C = 1$ in (27), we see that the results in both Figures 5 and 6 are consistent with a value of A in (1) of about 0.7 to 5, and a value of α of about 1/2, and that the results are not very sensitive to the value of K_2 . *Jobson et al.* [1999] present results from two other aircraft programs in addition to the ABLE 3 data points plotted in Figures 5 and 6 that collected samples of a suite of species of varying lifetimes from aircraft flying extended tracks at

various levels in the troposphere. The species lifetimes varied from about 4 days to about 4×10^4 days. The results for tropospheric measurements (PBL to 12 km) are as follows: For the ABLE 3B, $A = 1.6$ and $\alpha = 0.46$; for the Transport and Atmospheric Chemistry Near the Equator-Atlantic (TRACE-A), $A = 2.9$ and $\alpha = 0.52$; for the PEM in the Western Pacific Ocean Phase B (PEM-West B), $A = 4.3$ and $\alpha = 0.53$. We see that the results generally agree with the model predictions.

4.2. Mean Scalar Concentration

[42] This model can also be used to formulate a relationship among the mean PBL (or lower troposphere) concentration, surface flux, and lifetime of a trace reactive species. That is, if any two of these variables are known, the model can predict the third. To develop this relation, we solve for the ratio of the species concentration in the PBL to the surface flux, and normalize by the PBL depth z_1 and the lifetime τ . Thus, if the species were confined to the PBL, that is, if $w_{12} = 0$, then the species concentration for this case, defined by $S_1|_{PBL}$ would be

$$S_1|_{PBL} = \frac{F_0 \tau}{z_1}. \quad (28)$$

The ratio of the model prediction of S_1 to (28) gives

$$\frac{S_1}{S_1|_{PBL}} = \frac{S_1 z_1}{F_0 \tau}. \quad (29)$$

We can similarly solve for the normalized mean concentration in the free atmosphere just above the PBL to obtain the normalized concentration, $S_2(z_1)z_1/(F_0 \tau)$.

[43] These relations are plotted in Figure 7. The results show that, as expected, as $\tau \rightarrow 0$, $S_1 z_1/(F_0 \tau) \rightarrow 1$, since only a small amount leaks out of the PBL, and for $\tau > 100$ days (for $K_2 = 10 \text{ m}^2 \text{ s}^{-1}$), or 1000 days (for $K_2 = 1 \text{ m}^2 \text{ s}^{-1}$), $S_1 z_1/(F_0 \tau)$ starts to flatten out, due to buildup of significant concentrations throughout the atmosphere. As an example of the effect on mean concentration, for two species, a , b having the same surface flux and with $K_2 = 10 \text{ m}^2 \text{ s}^{-1}$ but

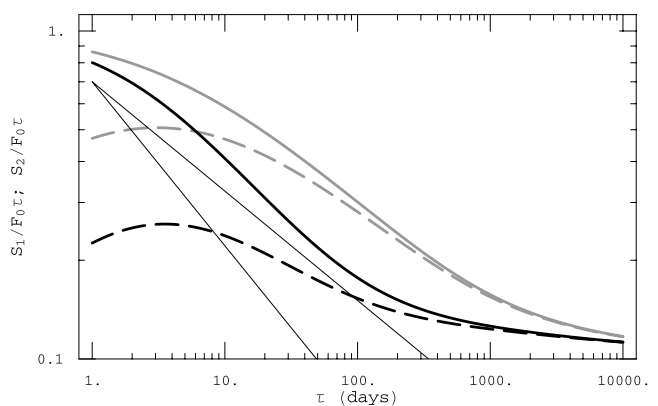


Figure 7. Normalized concentrations in the PBL $S_1 z_1/(F_0 \tau)$ (thick solid line) and just above the PBL $S_2(z_1) z_1/(F_0 \tau)$ (thick dashed line) for $K_2 = 10 \text{ m}^2 \text{ s}^{-1}$ (black lines) and for $K_2 = 1 \text{ m}^2 \text{ s}^{-1}$ (gray lines). The thin reference lines have slopes of $-1/2$ and $-1/3$.

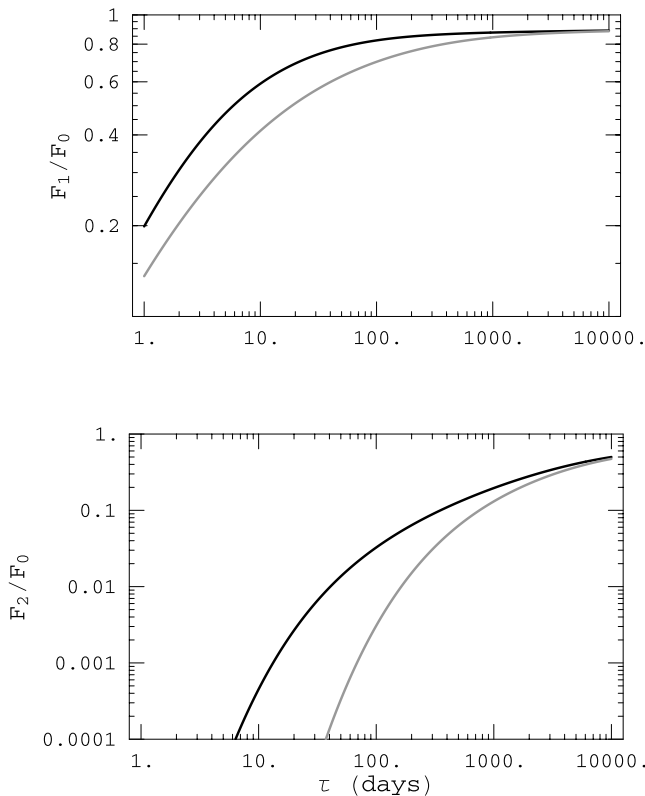


Figure 8. Flux at the PBL top F_1/F_0 (top panel) and the tropopause F_2/F_0 (bottom panel) normalized by the surface flux F_0 plotted versus lifetime τ for values of $K_2 = 10 \text{ m}^2 \text{ s}^{-1}$ (black lines) and $K_2 = 1 \text{ m}^2 \text{ s}^{-1}$ (gray lines).

with $\tau_a = 10$ days and $\tau_b = 100$ days, the concentration in the PBL $S_{1b} \approx 4.5 S_{1a}$, and the concentration just above the PBL, $S_{2b} \approx 6.2 S_{2a}$.

[44] Interestingly, the value of $S_2(z_1)z_1/(F_0\tau)$ peaks at $\tau \approx 3$ days; for shorter times, the species is destroyed too quickly to build up a concentration at $S_2(z_1)$, while for longer times, the species “leaks” away to higher levels.

[45] We can also calculate the ratios of the fluxes at the two interfaces to the surface flux (Figure 8). The PBL top flux decreases below 50% for $\tau \leq 5$ and 18 days (for $K_2 = 10$ and $1 \text{ m}^2 \text{ s}^{-1}$). At the tropopause, the flux decreases below 50% for $\tau \leq 28$ and 34 years (for $K_2 = 10$ and $1 \text{ m}^2 \text{ s}^{-1}$). Another way to look at this is that the ratio of the two lifetimes for the same decrease in the ratio of the flux at the tropopause to the flux at the PBL top is of order 10^3 .

5. Conclusions

[46] The three-layer vertical diffusion model presented here is very different from the earlier conceptual models that assumed single-layer structure and related fluctuations to horizontal variability in emissions. Here we assume horizontal homogeneity and relate fluctuations in the PBL and the overlying free troposphere to entrainment across the PBL top and the tropopause, and concentration difference across the free troposphere. We obtain a τ dependency of σ_s/S_1 and a fluctuation magnitude that are similar to observations obtained from large-scale airborne sampling programs. Furthermore, the model predicts how the mean

concentration and flux change as a function of height for a specified species lifetime.

[47] Because of the simplicity of the model, it is relatively straightforward to extend it to more complicated situations such as time-dependent emission rates or vertical variations in lifetime, or more sophisticated formulations for vertical diffusion. It would also be interesting to compare the predictions of this model for both mean and standard deviations with long-term observations from remote sites.

[48] **Acknowledgments.** This research was partially supported under NASA PEM-Tropics order L68847D. Discussions with Jonah Colman, Don Blake, and Nicola Blake were very helpful. The reviews by Leif Kristensen, Gao Chen, and Ian Faloon led to several improvements in the paper. The National Center for Atmospheric Research is sponsored by the National Science Foundation.

References

- Birner, T., A. Dörnbrack, and U. Schumann, How sharp is the tropopause at midlatitudes?, *Geophys. Res. Lett.*, 29(14), 1700, doi:10.1029/2002GL015142, 2002.
- Colman, J. J., D. R. Blake, and F. S. Rowland, Atmospheric residence time of CH_3Br estimated from the Junge spatial variability relation, *Science*, 281, 392–396, 1999.
- Cotton, W. R., G. D. Alexander, R. Hertenstein, R. L. Walko, R. L. McAnelly, and M. Nicholls, Cloud venting: A review and some global annual estimates, *Earth Sci. Rev.*, 39, 169–206, 1995.
- Danielsen, E. F., A dehydration mechanism for the stratosphere, *Geophys. Res. Lett.*, 9, 605–608, 1982.
- Danielsen, E. F., In situ evidence of rapid, vertical irreversible transport of lower tropospheric air into the lower tropical stratosphere by convective cloud turrets and by larger-scale upwelling in tropical cyclones, *J. Geophys. Res.*, 98, 8665–8681, 1993.
- Ehhalt, D. H., F. Rohrer, A. Wahner, M. J. Prather, and D. R. Blake, On the use of hydrocarbons for the determination of tropospheric OH concentrations, *J. Geophys. Res.*, 103, 18,981–18,997, 1998.
- Gibbs, A. D., and W. G. N. Slinn, Fluctuations of trace gas concentrations in the troposphere, *J. Geophys. Res.*, 78, 574–576, 1973.
- Hamrud, M., Residence time and spatial variability for gases in the atmosphere, *Tellus, Ser. B*, 35, 295–303, 1983.
- Holton, J. R., P. H. Haynes, M. E. McIntyre, A. R. Douglass, R. B. Rood, and L. Pfister, Stratosphere–troposphere exchange, *Rev. Geophys.*, 33, 403–439, 1995.
- Hunten, D. M., Vertical transport in atmospheres, in *Atmospheres of Earth and the Planets*, edited by B. M. McCormac, pp. 59–72, D. Reidel, Norwell, Mass., 1975.
- Jaenicke, R., Physical aspects of the atmospheric aerosol, in *Chemistry of the Polluted and Unpolluted Troposphere*, edited by H. W. Georgi and W. Jaschke, pp. 341–373, D. Reidel, Norwell, Mass., 1982.
- Jobson, B. T., D. D. Parrish, P. Goldan, F. C. Fehsenfeld, D. R. Blake, N. J. Blake, and H. Niki, Spatial and temporal variability of nonmethane hydrocarbon mixing ratios and their relation to photochemical lifetime, *J. Geophys. Res.*, 103, 13,557–13,567, 1998.
- Jobson, B. T., S. A. McKeen, D. D. Parrish, F. C. Fehsenfeld, D. R. Blake, A. H. Goldstein, S. M. Schauffler, and J. Elkins, Trace gas mixing ratio variability versus lifetime in the troposphere and stratosphere: Observations, *J. Geophys. Res.*, 104, 16,091–16,113, 1999.
- Junge, C. E., *Air Chemistry and Radioactivity*, Academic, San Diego, Calif., 1963.
- Junge, C. E., Residence time and variability of tropospheric trace gases, *Tellus*, 26, 477–488, 1974.
- Kimmel, S., J. Wyngaard, and M. Otte, “Log-chipper” turbulence in the convective boundary layer, *J. Atmos. Sci.*, 59, 1124–1134, 2002.
- Lenschow, D. H., Micrometeorological techniques for measuring biosphere–atmosphere trace gas exchange, in *Biogenic Trace Gases: Measuring Emissions from Soil and Water*, edited by P. A. Matson and R. C. Harriss, pp. 126–163, Blackwell Sci., Malden, Mass., 1995.
- Lenschow, D. H., I. Paluch, A. Bandy, D. Thornton, D. Blake, and I. Simpson, Use of a mixed-layer model to estimate dimethyl sulfide flux and application to other trace gas fluxes, *J. Geophys. Res.*, 104, 16,275–16,295, 1999.
- Levin, I. B., and V. Hesshaimer, Refining of atmospheric transport model entries by the globally observed passive tracer distributions of $^{85}\text{krypton}$ and sulfur hexafluoride (SF_6), *J. Geophys. Res.*, 101, 16,745–16,755, 1996.

- Liley, J. B., Analytic solution of a one-dimensional equation for aerosol and gas dispersion in the stratosphere, *J. Atmos. Sci.*, 52, 3283–3288, 1995.
- Massie, S. T., and D. M. Hunten, Stratospheric eddy diffusion coefficients from tracer data, *J. Geophys. Res.*, 86, 9859–9868, 1981.
- Moeng, C.-H., and J.-C. Wyngaard, Evaluation of turbulent transport and dissipation closures in second-order modeling, *J. Atmos. Sci.*, 46, 2311–2330, 1989.
- Olofsson, M., Global vertical mass transport by clouds: A two-dimensional model study, Tech. Rep. CM-74, Int. Meteorol. Inst., Stockholm, 1988.
- Sellers, W. D., *Physical Climatology*, Univ. of Chicago Press, Chicago, Ill., 1965.
- Slinn, W. G. N., A simple model for Junge's relationship between concentration fluctuations and residence times for tropospheric trace gases, *Tellus, Ser. B*, 40, 229–232, 1988.
- Telegadas, K., and G. Ferber, Atmospheric concentrations and inventory of krypton-85 in 1973, *Science*, 190, 882–883, 1975.
- Tennekes, H., A model for the dynamics of the inversion above a convective boundary layer, *J. Atmos. Sci.*, 30, 558–567, 1973.
- Tennekes, H. and J. L. Lumley, *A First Course in Turbulence*, MIT Press, Cambridge, Mass., 1972.
- Wyngaard, J. C., and R. A. Brost, Toward convective boundary layer parameterization: A scalar transport module, *J. Atmos. Sci.*, 41, 102–112, 1984.
-
- D. Gurarie, Department of Mathematics, Case Western Reserve University, Cleveland, OH 44106, USA.
- D. H. Lenschow, National Center for Atmospheric Research (NCAR), P.O. Box 3000, Boulder, CO 80307-3000, USA. (lenschow@ncar.ucar.edu)